Eur. Phys. J. D **38**, 193–197 (2006)
DOI: 10.1140/epjd/e2006-00019-1

THE EUROPEAN PHYSICAL JOURNAL D

The electronic structure and magnetic property of μ-hydroxo bridged manganese porphyrin dimer

K. Koizumi[a], M. Shoji, Y. Kitagawa, H. Ohoyama, T. Kasai, and K. Yamaguchi

Department of Chemistry, Graduate School of Science, Osaka University, Toyonaka, Osaka 560-0043, Japan

Received 6 August 2005
Published online 31 January 2006 –

Abstract. The electronic structure and effective exchange integrals (J_{ab}) between two manganese (III) ions of porphyrin dimer (PPMn(III)–OH–Mn(III)PP) were examined by using unrestricted hybrid DFT (UHDFT) methods. The dependence of J_{ab} on bond angle between two manganese ($\angle$ Mn–OH–Mn) is also calculated to elucidate orbital overlap effect for J_{ab} value in the system. Natural orbital analysis is performed to explain the overlap effect in terms of the instability of the π, σ and δ orbitals by using diradical character.

PACS. 31.15.Ar Ab initio calculations – 31.15.Ew Density-functional theory

1 Introduction

Manganese complexes and clusters have been one of the attractive substances in molecular science. Manganese ion can take various oxidation numbers and can be seen in various systems such as the photosynthesis, which uses a cluster of manganese in the cell of plants. This cluster uses the energy of light to make oxygen from water. The remarkable points of this reaction are (1) effective exchange of energy of light and electron (2) efficient transportation of the energy (3) cleavage of the stable chemical bond of water under the modest condition. But the detail of the structure and the reaction of the cluster are still unknown.

On the other hand, porphyrin complexes can be seen in many biological systems. The most outstanding system may be hemoglobin which include iron ion. When iron ion adsorbs an oxygen molecule, the porphyrin ligand change its structure and iron ion changes its spin state from high spin state to low spin state.

Naruta et al. reported that a binuclear Mn porphyrin complex could lead to oxygen evolution from water [1,2]. An essential feature of their proposed mechanism is the formation of hydroxide and oxide complexes with the manganese porphyrin dimer. Although the electronic structure and the interaction between manganese centers are considerably interesting, the synthesis and well-defined characterization of manganese complexes with simple bridging ligand systems do not have been reported so many. Naruta et al. speculated that the reaction undergoes PPMn–$(OH)_2$–MnPP, PPMn–O–O–MnPP etc. However, the structures of the intermediates dose not have been obtained experimentally.

[a] e-mail: koizumi@chem.sci.osaka-u.ac.jp

On the other hand, magnetic properties of manganese porphyrin complex have been of some interest in the field of molecular magnetism. The manganese in the complex have localized spins, so the electron transfer complex such as PPMn–TCNE–MnPP shows the nature of a molecular magnet [3]. The magnetic parameters such as J_{ab} are very sensitive to the electronic structure of the complex. Therefore, J_{ab} can be the good clue to elucidate the electronic structure of the complex.

Cheng et al. succeed to obtain μ-hydroxo bridged manganese porphyrin crystal [4]. They measure the J_{ab} values experimentally and concluded that the complex exhibited antiferromagnetic behavior. This complex may give good suggestion to the investigation of the intermediates of Naruta's reaction. To elucidate the oxygen evolution reaction, we have calculated the electronic structure of Cheng's complex theoretically.

In our previous work [5], however, the reduced model of Cheng's complex was studied but the effect of bond angle and bridged type (O or OH) was not made clear.

In this work, we use μ-hydroxo bridged manganese porphyrin dimer (PPMn–OH–MnPP) and deduce effective exchange integrals from ab initio calculation methods using UHDFT (UB3LYP and UB2LYP [6,7]). By using the ab initio calculation, we discussed the effect of bridging angle and bridging species.

2 Theoretical background

2.1 UHDFT

There are mainly two different types of theoretical descriptions in molecular orbital (MO) i.e symmetry-adapted (SA) [8] and broken-symmetry (BS) approaches [9].

The former approaches including configuration interaction (CI), CASSCF, and related MR perturbation theories are desirable for accurate description of strong electron correlation systems. But their applicability is limited to small molecular systems because of computing cost. On the other hand, the latter such as unrestricted Hartree-Fock (UHF) and spin-polarized DFT (UDFT) can be easily applied to large systems because of a single Slater determinant. The Kohn-Sham density functional theory is one of the most popular approaches in computational chemistry [10]. The fundamental concept of KS–DFT is non-interacting picture under the effective potential. The energy expression is as follows.

$$E = T_0[\{\psi_i\}] + V_{ne}[\rho] + V_{clmb} + E_{XC}[\rho] \tag{1}$$

where T_0, V_{ne}, and V_{clmb} are the kinetic energy of non-intersecting electrons, nuclear-attraction energy, and the classical Coulomb term, respectively. The one of the extensions of KS-DFT is a hybrid type DFT (HDFT) involving the HF exchange term. E_{XC} is defined as

$$E_{XC} = C_1 E_X^{HF} + C_2 E_X^{Slater} + C_3 E_X^{Becke} + C_4 E_C^{VWN} + C_5 E_C^{LYP} \tag{2}$$

where E_X^{HF}, E_X^{Slater}, and E_X^{Becke} are exchange term of HF, Slater, and Becke [11] respectively. E_C^{VWN} and E_C^{LYP} are VWN [12] and LYP [13] correlation terms. $\{C_i\}_{i=1-5}$ are the hybrid parameters. B3LYP parameters are given by 0.2, 0.8, 0.72, 1.0, 0.81 and UB2LYP ones are given by 0.5, 0.5, 0.5, 1.0, 1.0, respectively. Here, UB2LYP is a magnetic effective density functional (MEDF) method [6], of which the hybrid parameter $C_1 = 0.5$ and it is equivalent to Becke's so-called Half and Half LYP method.

2.2 Natural orbital analysis

To obtain a basic picture of MOs, the natural orbitals (NOs) of SA and BS solutions were determined by diagonalizing their spin-traced first-order density matrices γ [14] as

$$\gamma(\mathbf{r}, \mathbf{r}') = \sum_i n_i \phi_i(\mathbf{r}) \phi_i^*(\mathbf{r}') \tag{3}$$

where n_i denotes the occupation number of an NO ϕ_i that lies in the range $0 \leq n_i \leq 2$. The spin-polarized MOs ψ_i^+ and ψ_i^- for the up and down spins can be expressed as

$$\psi_i^{\pm} = \cos\theta_i \phi_i \pm \sin\theta_i \phi_i^* \quad (i = 1, 2, \cdots N) \tag{4}$$

where θ_i is the orbital mixing parameter and N is the number of bonding natural orbitals. The orbital overlap T_i between the corresponding orbitals is defined as a measure of orbital splitting by

$$T_i = \langle \psi_i^+ | \psi_i^- \rangle = \cos 2\theta_i \tag{5}$$

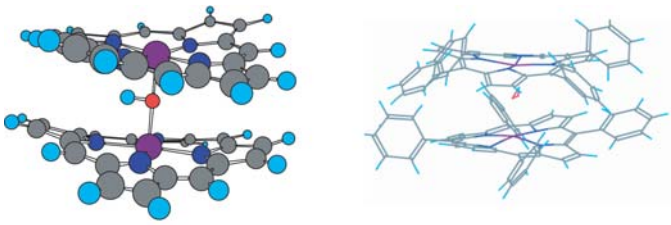

Fig. 1. Calculated model complex of μ-hydroxo bridged manganese dimer (PPMn–OH–MnPP) is (a) and X-ray structure of $\{[Mn(TPP)]_2OH\}^+$ (TPP = tetraphenylporphinato) is (b).

where T_i is 1.0 for closed-shell systems ($\theta_i = 0$) and $0 \leq T_i < 1.0$ for open-shell systems ($\theta_i > 0$). The occupation number of the bonding and antibonding NOs are expressed by the orbital overlap T_i [15]:

$$n_i = 1 + T_i, \qquad n_i^* = 1 - T_i. \tag{6}$$

2.3 Effective exchange integrals

The UB2LYP and UB3LYP calculations were performed to examine a dependency of the effective exchange interactions between Mn(III) ions on the computational methods

$$H = -2J_{ab} S_a S_b \tag{7}$$

where S_c ($c = a, b$) denotes the spin at site c and J_{ab} is effective exchange integral. The effective exchange integrals (J_{ab}) are calculated from the difference of total energies and $\langle S^2 \rangle$ between high-spin and low-spin by using our approximate spin projection (AP) scheme [16]

$$J_{ab} - \frac{{}^{LS}\langle \hat{H} \rangle_{UDFT} - {}^{HS}\langle \hat{H} \rangle_{UDFT}}{{}^{HS}\langle S^2 \rangle_{UDFT} - {}^{LS}\langle S^2 \rangle_{UDFT}}. \tag{8}$$

2.4 Reduced model complex

To elucidate the electronic structure of μ-hydroxo bridged porphyrin dimer, we constructed model complex of μ-hydroxo bridged manganese dimer (PPMn–OH–MnPP) as shown in Figure 1a together with X-ray structure of $\{[Mn(TPP)]_2OH\}^+$ (TPP = tetraphenylporphinato) as illustrated in Figure 1b.

In the model complex, the bond angle θ between two manganese ($\angle$ Mn–OH–Mn) is verified. To reduce calculation cost, the eight phenyl groups attached to the porphyrin rings were removed.

2.5 Computational details

The Huzinaga's MIDI+P basis set (533(21)/53(21)/(41)) was used for Mn(III) ion and the 6–31G* basis set was used for other atoms [17]. All coordination was taken from X-ray crystallographic data. All calculation were performed by using Gaussian 98 program package [18].

Table 1. Total energies and $\langle S^2 \rangle$ values of HS and LS of Mn–OH–Mn, and effective exchange integrals (J_{ab}) values calculated by UB2LYP, and UB3LYP.

method	LS state		HS state		
	Energy, a.u.	$\langle S^2 \rangle$	Energy, a.u.	$\langle S^2 \rangle$	J_{ab}, cm^{-1}
UB3LYP	–4353.93018057	3.9194	–4353.91692796	20.0935	179.8
UB2LYP	–4352.57444237	4.0362	–4352.56709347	20.1041	100.4

Table 2. Spin and charge densities calculated by UB2LYP, and UB3LYP.

	spin density		charge density	
methods	LS	HS	LS	HS
UB3LYP				
Mn	3.82	3.92	1.24	1.26
O	–0.02	0.31	–0.86	–0.90
H	0.00	0.00	0.48	0.48
Mn	–3.82	3.90	1.26	1.28
UB2LYP				
Mn	3.97	4.01	1.49	1.50
O	–0.02	0.26	–1.01	–1.03
H	0.00	0.00	0.51	0.51
Mn	–3.95	4.00	1.51	1.52

3 Result and discussion

3.1 J_{ab} value of reduced model

The effective exchange integrals (J_{ab}) of μ-hydroxo model complex ($\angle$ Mn–OH–Mn = 180) are calculated by using formula (8) as summarized in Table 1. Total energies and $\langle S^2 \rangle$ of two state (high spin ($s = 8/2$)) and low spin ($s = 0$)) are also presented in the table. In case of Mn–O–Mn, the J_{ab} value of μ-oxo cases are –290.9 cm^{-1} for UB3LYP, and –157.6 cm^{-1} for UB2LYP, respectively [5]. The absolute value of J_{ab} of PPMn–OH–MnPP is smaller than that of PPMn–O–MnPP.

On the other hand, the antiferromagnetic interaction between two Mn(III) of {[Mn(TPP)]$_2$OH} (TPP = tetraphenylporphinato) is reported as –35.5 cm^{-1} [4]. Therefore, the absolute value of J_{ab} of PPMn–OH–MnPP is still larger than experimental one. However there is the tendency that μ-hydroxo bridged type shows weaker antiferromagnetic interaction than μ-oxo one.

3.2 Spin and charge density

Spin and charge densities by two methods, namely UB3LYP and UB2LYP are shown in Table 2. In the table, the magnitude for α spin ($S = 1/2$) and β spin ($S = -1/2$) are defined to be 1.0 and –1.0, respectively. Charge and spin densities are distributed symmetrically according to the symmetry of the model. The charge density populations on manganese do not correspond to its formal charge +3, but about +1.5, which shows the electron donations from the porphyrin ring.

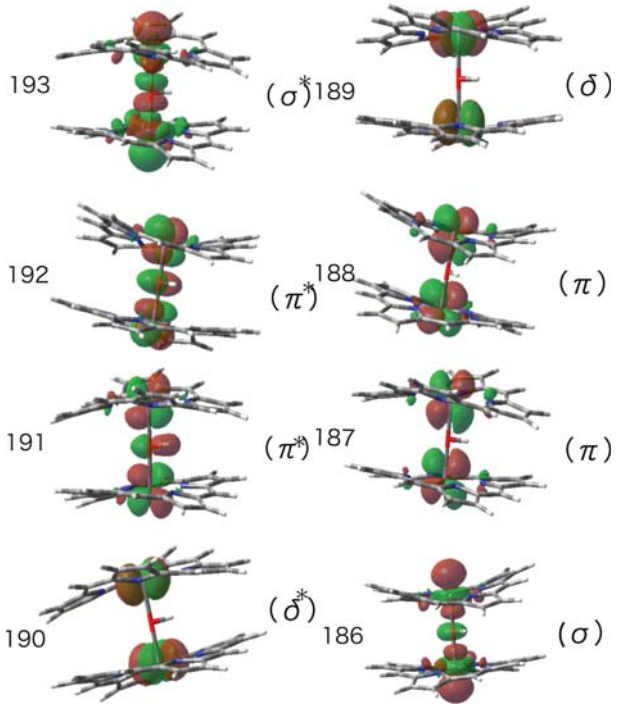

Fig. 2. The pictures of natural orbitals of Mn–OH–Mn. The bond angle ($\angle$ Mn–OH–Mn) is 180°.

Table 3. Occupation number, and T values of LS state calculated by UB2LYP.

orbital no.	occupation number	T
193	0.79	
192	0.90	
191	0.94	
190	1.00	
189	1.00	0.00
188	1.06	0.06
187	1.10	0.10
186	1.21	0.21

3.3 Natural orbital analysis

To elucidate the orbital interaction schemes in PPMn–OH–MnPP as illustrated in Figure 2, the natural orbital analyses of the low-spin UHDFT solutions was carried out. Table 3 shows their occupation numbers and T values in case of UB2LYP. From the picture of Figure 2, we found that NOs of magnetic orbital were localized on Mn–OH–Mn. This suggests large energy gaps between Mn–OH–Mn orbitals and PP ring orbital. The shapes and order of

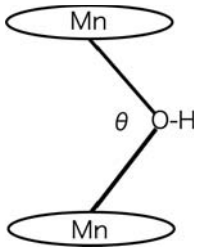

Fig. 3. The schematic view of bond angle.

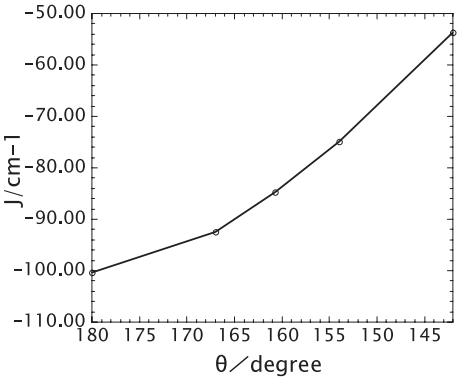

Fig. 4. The dependence of J_{ab} on the bond angle. The calculation method is UB2LYP. The bond angle plotted are 180°, 167°, 160°, 154°, and 142°.

NOs of the PPMn–O–MnPP are similar to ones of Mn–OH–Mn [5]. The occupation numbers show that bonding interactions are weak even for σ-type magnetic orbitals. This tendency suggests that spins on Mn(III) ion are almost localized.

3.4 Dependence of J_{ab} on bond angle

As mentioned above, the J_{ab} value of μ-hydroxo model complex (Mn–OH–Mn) became smaller than that of μ-oxo (Mn–O–Mn). However the J_{ab} value of μ-hydroxo was still larger than that of experimental one. The model structures did not consider the effect of the bent angle between Mn–OH–Mn (expt = 160.7°) [5]. Figure 3 illustrates the bent between Mn–OH–Mn.

The dependence of J_{ab} on the bond angle by using UB2LYP is shown in Figure 4. The bond angle plotted in the figure are 180°, 167°, 160°, 154°, and 142°. As the bond angle decrease, absolute value of J_{ab} becomes small. The experimental ∠ Mn–OH–Mn is 160.7° and the calculation result of J_{ab} at the plotted point of 160° is still larger than experimental one. However, by considering the effect of bond angle, calculated J_{ab} value becomes close to the experimental one.

The natural orbitals in case of 160° are depicted in Figure 5. The tendency of their shapes are similar to those of reduced model complex such as Mn–O–Mn and Mn–OH–Mn (bond angle 180°).

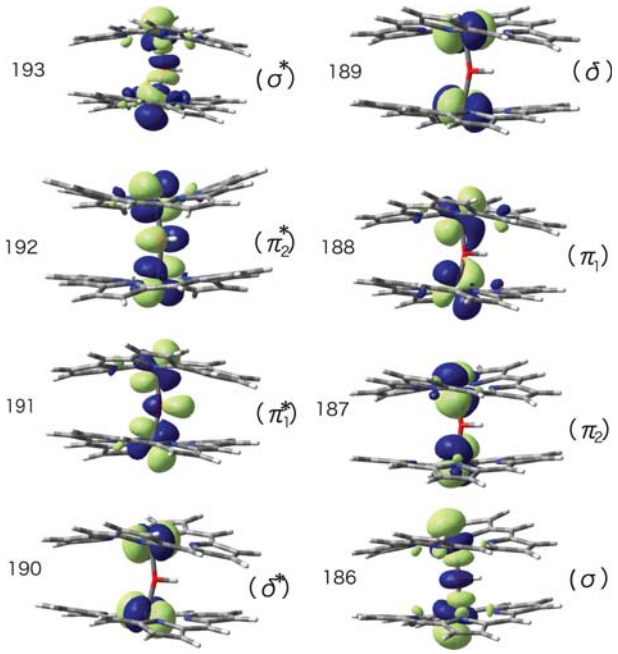

Fig. 5. Natural orbitals in case of 160°.

3.5 Occupation number and diradical character

Spin source of the system is the d-orbitals in Mn(III). Occupation numbers of magnetic orbitals show bonding and non-bonding interactions between the spins on Mn ions through the O^{2-} and HO^{-}. To clarify the stability of the magnetic orbitals, diradical character is introduced. The formula of diradical character is as follows

$$Y_i = \frac{n_i^2 - 4n_i + 4}{n_i^2 - 2n_i + 2} \tag{9}$$

where Y_i is diradical character and n_i is the occupation number of each type of natural orbitals (σ, π, and δ) respectively. The diradical character is usually shown in percentage. If n_i is 1.0, diradical character is 100% (localized radical) and if n_i is 2.0, diradical character is 0% (covalent bond). Y_i indicates the instability of the magnetic orbital in other words it works as an index of non-bonding character. If diradical character is large, non-bonding character of the orbital is strong. Occupation numbers and diradical characters in case of Mn–O–Mn, Mn–OH–Mn (∠ Mn–OH–Mn = 180°), and bent model of Mn–OH–Mn (∠ Mn–OH–Mn = 160°) are summarized in Table 4.

As illustrated in Figure 5, π_1 orbital is on the OH axis. The diradical characters of π_1, π_2, and σ orbitals of Mn–OH–Mn become larger than those of Mn–O–Mn. However, diradical characters of δ is constant (100%). The diradical character of π_1 orbital increase drastically. It shows that the bonding interaction i.e. antiferromagnetic coupling of this π-type orbital at the bridge of Mn–OH–Mn is weaker than that of Mn–O–Mn. The bridging ligand OH makes the antiferromagnetic interaction between Mn–X–Mn weaker. Therefore, absolute value of J_{ab} of Mn–OH–Mn is smaller than that of Mn–O–Mn. The increase of diradical character of π and σ orbitals of bent model in

Table 4. The occupation number and diradical character. The values in parentheses are diradical character. The calculation method is UB2LYP. The π_1 is π-type orbital which is on the OH axis.

	Mn–O–Mn	Mn–OH–Mn (180°)	Mn–OH–Mn (160°)
δ	1.00(100%)	1.00 (100%)	1.00 (100%)
π_1	1.17 (67%)	1.06 (88%)	1.04 (92%)
π_2	1.17 (67%)	1.10 (80%)	1.09 (82%)
σ	1.27 (50%)	1.21 (60%)	1.19 (63%)

comparison with linear model indicates that the absolute value of J_{ab} of bent model becomes smaller.

4 Conclusions

We examined the electronic structure and magnetic property of the model complex of $\{[Mn(TPP)]_2OH\}^+$ using UHDFT calculation in terms of two points as follows. One is the chemical species of bridge ligand of PPMn–X–MnPP (X = O or OH), and the other is the bent angle between Mn–X–Mn. OH bond of bridging ligand and bent angle decreased the overlap between α and β spins on two Mn(III) ions. However, calculated J_{ab} values were still larger than experimental one. Therefore another factor except for ligand species and bent angle must be considered to explain experimental J_{ab} value.

From the results, two Mn(III) ions showed weak interaction with HO^- or O^{2-} in contrast to Naruta's complex, which decompose water to oxygen. Similar to active site of photosynthesis consisted of Mn cluster, it have been reported that high valence Mn(V) ion promoted the reaction. On the other hand, the existence of high valence Mn(V)–PP complex dose not have been obtained experimentally. Theoretical analyses of the electronic structure of high valence Mn(V)–PP is now in progress.

This work has been supported by Grants-in-Aid for Scientific Research on Priority Areas (Nos. 16750049 and 14204061) from Ministry of Education, Culture, Sports, Science and Technology, Japan. K.K is also supported by Research Fellowships of the Japan Society for the Promotion of Science for Young Scientists.

References

1. Y. Naruta, M. Sasayama, T. Sasaki, Angew. Chem. Int. Ed. Engl. **33**, 1839 (1994)
2. Y. Naruta, *Seibutu to kinzoku* (Kuba pro, Tokyo, 2001), p. 70 (in Japanese)
3. K. Koizumi, M. Shoji, Y. Kitagawa, T. Taniguchi, T. Kawakami, M. Okumura, K. Yamaguchi, Polyhedron **24**, 2720 (2005)
4. B. Chang, F. Cukiernik, P.H. Fries, J.C. Marchon, W.R. Scheidt, Inorg. Chem. **34**, 4627 (1995)
5. K. Koizumi, M. Shoji, Y. Nishiyama, Y. Maruno, Y. Kitagawa, T. Soda, S. Yamanaka, M. Okumura, K. Yamaguchi, Int. J. Quant. Chem. **100**, 943 (2004)
6. Y. Kitagawa, T. Soda, Y. Shigeta, S. Yamanaka, Y. Yoshioka, K. Yamaguchi, Int. J. Quant. Chem. **84**, 592 (2001)
7. Y. Kitagawa, T. Kawakami, K. Yamaguchi, Mol. Phys. **100**, 1829 (2002)
8. K. Yamaguchi, K. Ohta, S. Yabushita, T. Fueno, Chem. Phys. Lett. **49**, 555 (1977)
9. J.K. Labanowski, J.W. Andzelm, *Density Functional Methods in Chemistry* (Springer, New York, 1991)
10. R.G. Parr, W. Yang, *Density Functional Theory of Atoms and Molecules* (Oxford University Press, New York, 1989)
11. A. Becke, Phys. Rev. A **38**, 3098 (1988)
12. S.H. Vosko, L. Wilk, M. Nusair, Can. J. Phys. **58**, 1200 (1980)
13. C. Lee, W. Yang, R.G. Parr, Phys. Rev. B **37**, 785 (1988)
14. K. Yamaguchi, M. Okumura, K. Takeda, S. Yamanaka, Int. J. Quant. Chem. **27**, 5011 (1993)
15. M. Nishio, Y. Yoshioka, K. Yamaguchi, K. Mashima, K. Tani, A. Nakamura, J. Phys. Chem. A **101**, 705 (1997)
16. K. Yamaguchi, Y. Takahara, T. Fueno, Appl. Quant. Chem. 155 (1986)
17. K. Yamaguchi, Chem. Phys. Lett. **68**, 477 (1979)
18. M.J. Frisch, G.W. Trucks, H.B. Schlegel, G.E. Scuseria, M.A. Robb, J.R. Cheeseman, V.G. Zakrzewski, J.A. Montgomery Jr, R.E. Stratmann, J.C. Burant, S. Dapprich, J.M. Millam, A.D. Daniels, K.N. Kudin, M.C. Strain, O. Farkas, J. Tomasi, V. Barone, M. Cossi, R. Cammi, B. Mennucci, C. Pomelli, C. Adamo, S. Clifford, J. Ochterski, G.A. Petersson, P.Y. Ayala, Q. Cui, K. Morokuma, D.K. Malick, A.D. Rabuck, K. Raghavachari, J.B. Foresman, J. Cioslowski, J.V. Oritz, B.B. Stefanov, G. Liu, A. Liashenko, P. Piskorz, I. Komaromi, R. Gomperts, R.L. Martin, D.J. Fox, T. Keith, M.A. Al-Laham, C.Y. Peng, A. Nanayakkara, C. Gonzalez, M. Challacombe, P.M.W. Gill, B. Johnson, W. Chen, M.W. Wong, J.L. Andres, M. Head-Gordon, E.S. Replogle, J.A. Pople, Gaussian 98, Gaussian Inc, Pittsburgh, PA (1998)